Compressive Imaging

Albert Fannjiang, **UC Davis**

Outline

- Review: inverse scattering
- Review: compressed sensing
- Random incident and scattering directions: SIMO, SISO
- Random illumination
- Resolution and superresolution
- MUSIC: thresholding, noise tolerance.

Inverse scattering

- Plane wave incidence

$$u^{\mathsf{i}}(\mathbf{r}) = e^{i\omega \mathbf{r}\cdot\widehat{\mathbf{d}}}, \quad \mathbf{r} \in \mathbb{R}^d$$

where $\widehat{\mathbf{d}} \in S^{d-1}, d = 2, 3$ is the incident direction.

$c_0 = 1$: $\omega =$ frequency/wavenumber.

- The scattered field $u^{\mathsf{s}} = u - u^{\mathsf{i}}$ then satisfies the Lippmann-Schwinger equation:

$$u^{\mathsf{s}}(\mathbf{r}) \;=\; \omega^2 \int_{\mathbb{R}^d} \nu(\mathbf{r}') \left(u^{\mathsf{i}}(\mathbf{r}') + u^{\mathsf{s}}(\mathbf{r}')\right) G(\mathbf{r}, \mathbf{r}') d\mathbf{r}'$$

where G is the Green function for the operator $-(\Delta + \omega^2)$.

- Measurement: scattered field (near field) or the scattering amplitude (far field).

- Far-field asymptotic: $d = 3$

$$\frac{e^{i\omega|\mathbf{r}-\mathbf{r}'|}}{4\pi|\mathbf{r}-\mathbf{r}'|} \approx \frac{e^{i\omega|\mathbf{r}|}}{4\pi|\mathbf{r}|} e^{-i\omega\hat{\mathbf{r}}\cdot\mathbf{r}'}.$$

Hence

$$u^{\mathsf{s}}(\mathbf{r}) = \frac{e^{i\omega|\mathbf{r}|}}{|\mathbf{r}|^{(d-1)/2}} \left(A(\hat{\mathbf{r}}, \hat{\mathbf{d}}) + \mathcal{O}\left(\frac{1}{|\mathbf{r}|}\right)\right), \quad \hat{\mathbf{r}} = \mathbf{r}/|\mathbf{r}|, \quad d = 2, 3$$

where the scattering amplitude A is determined by the formula

$$A(\hat{\mathbf{r}}, \hat{\mathbf{d}}) \;=\; \frac{\omega^2}{4\pi} \int_{\mathbb{R}^d} \nu(\mathbf{r}') u(\mathbf{r}') e^{-i\omega\mathbf{r}'\cdot\hat{\mathbf{r}}} d\mathbf{r}'.$$

- Born approximation

$$A(\hat{\mathbf{r}}, \hat{\mathbf{d}}) \;=\; \frac{\omega^2}{4\pi} \int_{\mathbb{R}^d} \nu(\mathbf{r}') u^{\mathsf{i}}(\mathbf{r}') e^{-i\omega\mathbf{r}'\cdot\hat{\mathbf{r}}} d\mathbf{r}'.$$

- Goal: determine ν from measurement data: A.

  Standard theory (Nachman, Novikov, Ramm, Sylvester-Uhlmann etc) of inverse scattering asserts the injectivity of the mapping from $\nu \in C_c^1$ with a nonnegative imaginary part to the corresponding scattering amplitude for a fixed frequency in three dimensions. That is, the refractive index can in principle be determined uniquely by the full knowledge of $A(\hat{\mathbf{r}}, \hat{\mathbf{d}}), \forall \hat{\mathbf{d}}, \hat{\mathbf{r}}$, for a fixed ω.

- Inverse problem: discrete vs. continuum.

  Finite data, finite number of pixels in computation domain.

  Issue of errors (external or model-mismatch).

Compressed sensing with RIP

- **Linear** inverse problem: $Y = \mathbf{\Phi} X + E$ where $\mathbf{\Phi}$ is an $n \times m$ matrix with

$$n \text{ (\# rows)} \ll m \text{ (\# columns)},$$

  i.e. severely underdetermined.

- Prior information: the target vector is sparse, $\|X\|_0 = s \sim n$.

  Difficulty: to identify the low dimensional subspace (the support space) out of $\binom{m}{n}$ *of them in a high dimensional vectors space.*

- Basis pursuit denoising or *Lasso*

$$\min_{Z \in \mathbb{C}^m} \|Z\|_1, \quad \text{s.t. } \|Y - \mathbf{\Phi} Z\|_2 \le \epsilon$$

  where ε is the size of error, i.e. $\|E\|_2 \le \varepsilon$.

  Recovery depends on RIP/incoherence property of $\mathbf{\Phi}$ and sparsity of X.

- Restricted isometry property (RIP): Define the restricted isometry constant (RIC) $\delta_s < 1, s \in \mathbb{N}$ to be the smallest positive number such that the inequality

$$(1-\delta_s)\|Z\|_2^2 \leq \|\Phi Z\|_2^2 \leq (1+\delta_s)\|Z\|_2^2$$

holds for all $Z \in \mathbb{C}^m$ of sparsity at most s.

Theorem 1 *(*Candès 08*)*

Suppose

$$\delta_{2s} < \sqrt{2} - 1.$$

Then the solution $\hat{X}$ of Lasso satisfies

$$\|\hat{X} - X\|_2 \;\leq\; C_1 s^{-1/2}\|X - X^{(s)}\|_1 + C_2\varepsilon$$

where $X^{(s)}$ is the best $s-$sparse approximation of X.

Examples: random i.i.d. matrices (no structure), random partial Fourier matrices (i.e. random row selections from DFT).

Theorem 2 *(*Rauhut 2008*)*

If

$$\frac{n}{\ln n} \geq C\delta^{-2} s \ln^2 s \ln m \ln \frac{1}{\gamma}$$

for $\gamma \in (0,1)$ *and some absolute constant* C*, then with probability at least* $1-\gamma$ *the random partial Fourier matrix satisfies the bound*

$$\delta_s \leq \delta.$$

DFT uses uniform sampling over the full Fourier domain.

Our scattering matrix is sampling only a small part of it.

Mutual coherence

- The mutual coherence

$$\mu(\Phi) = \max_{i \neq j} \frac{\left|\sum_k \Phi_{ik}^* \Phi_{kj}\right|}{\sqrt{\sum_k |\Phi_{ki}|^2}\sqrt{\sum_k |\Phi_{kj}|^2}}.$$

Proposition 1

$$\delta_s \leq \mu(s-1).$$

Sufficient condition for recovery

$$\mu(2s-1) \leq \sqrt{2}-1$$

or

$$s \leq \frac{1}{2}\left(1+\frac{\sqrt{2}-1}{\mu}\right).$$

Lower bound:

$$\mu \geq \sqrt{\frac{m-n}{n(m-1)}} \Rightarrow \frac{1}{\mu} = \mathcal{O}(\sqrt{n}).$$

Hence, by mutual coherence alone, we can recover

$$s = \mathcal{O}(\sqrt{n})$$

objects.

Operator norm

Theorem 3 (Candès-Plan 09) *Assume that* $E = (E_j) \in \mathbb{C}^n$ *and* $E_j, j = 1, ..., n$ *are i.i.d. complex Gaussian r.v.s with variance* σ^2 $(\varepsilon = \mathcal{O}(\sigma\sqrt{n}))$. *Suppose that*

$$\mu(\Phi) \le A_0 / \log m$$

and

$$s \le \frac{C_0 m}{\|\Phi\|^2 \log m}.$$

Assume

$$\min_i |X_i| > 8\sigma\sqrt{2\log m}.$$

Then the solution $\hat{X}$ *of*

$$\min_Z \frac{1}{2}\|Y - \Phi Z\|_2^2 + \sigma \cdot 2\sqrt{2\log m}\|Z\|_1$$

recovers the support of X *with high probability at least* $1 - 2m^{-1}((2\pi\log m)^{-}$ $sm^{-1}) - \mathcal{O}(m^{-2\log 2})$.

Typically,

$$\|\Phi\|^2 \sim \frac{m}{n} \quad \Rightarrow \quad s = \mathcal{O}(n/\log m).$$

Point scatterers

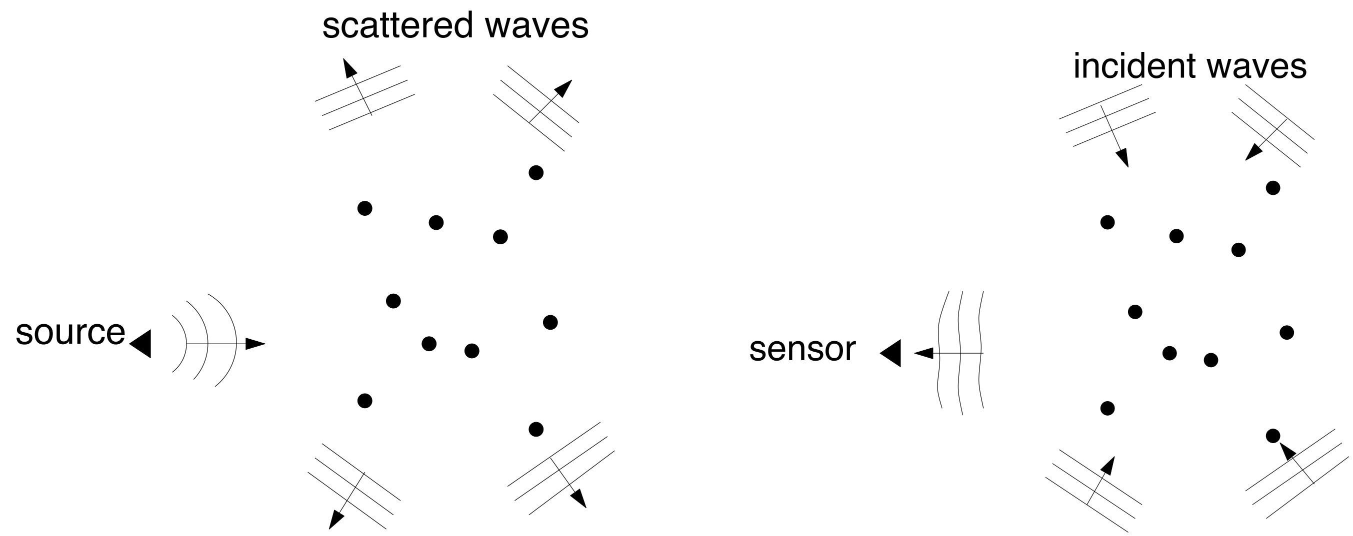

Reciprocity: SIMO $\sim$ multi-shot SISO measurement.

Assumption: point scatterers sit on a finite regular grid of spacing ℓ.

Measurement: randomly sample the scattering directions $\hat{\mathbf{r}}_l, l = 1, ..., n$.

SIMO (single-input-multiple-output)

The scattering amplitude is a finite sum

$$A(\hat{\mathbf{r}}_l, \hat{\mathbf{d}}) \;=\; \frac{\omega^2}{4\pi} \sum_{j=1}^{m} \nu_j u(\mathbf{r}_j) e^{-i\omega \mathbf{r}_j \cdot \hat{\mathbf{r}}_l}.$$

Excitation field $u(\mathbf{r}_i)$ satisfies the Foldy-Lax equation

$$u(\mathbf{r}_i) \;=\; u^{\mathrm{i}}(\mathbf{r}_i) + \omega^2 \sum_{i \neq j} G(\mathbf{r}_i, \mathbf{r}_j) \nu_j u(\mathbf{r}_j)$$

where all the multiple scattering effects are included but the self field is excluded to avoid blow-up.

Let $X = (\nu_j u(\mathbf{r}_j)) \in \mathbb{C}^m$. The (l, j)-entry of the sensing matrix is

$$e^{-i\omega(z_j \sin\tilde{\theta}_l + x_j \cos\tilde{\theta}_l)}$$

where $\tilde{\theta}_l$ is the sampling angle and $\mathbf{r}_j = (x_j, z_j)$ are grid points.

This is not the standard random partial Fourier matrix!

Coherence bound

Theorem 4 (AF 2009)

Suppose

$$m \leq \frac{\delta}{8} e^{K^2/2}, \quad \delta, K > 0.$$

Then the sensing matrix satisfies the coherence bound

$$\mu(\mathbf{\Phi}) < \chi^{\mathsf{s}} + \frac{\sqrt{2}K}{\sqrt{n}}$$

with probability greater than $(1-\delta)^2$ *where*

$$\chi^{\mathsf{s}} \leq c_t (1+\omega\ell)^{-1/2} \|f^{\mathsf{s}}\|_{t,\infty},$$

where $\|\cdot\|_{t,\infty}$ *is the Hölder norm of order* $t > 1/2$ *and the constant* c_t *depends only on* t*.*

For $d = 3$,

$$\chi^{\mathsf{s}} \leq c_1 (1+\omega\ell)^{-1} \|f^{\mathsf{s}}\|_{1,\infty}$$

If, however, $\text{supp}(f^{\mathsf{s}})$ *does not contains any Blind Spot, then* χ^{s} *satisfies the bound*

$$\chi^{\mathsf{s}} \le c_h (1+\omega\ell)^{-h} \|f^{\mathsf{s}}\|_{h,\infty}$$

where the constant c_h *depends only on* h.

- We do not need full view measurement: the support of f^{s} can be a small portion of $S^{d-1}, d = 2, 3$.

  We need some smoothness in f^{s}: a number of existing numerical tests (by others) neglect this!

- To have $\mu \ll 1$, need $\omega\ell \gg 1$ and $n \gg 1$.

- In the case of random partial Fourier matrix, $\chi^{\mathsf{s}} = 0$.

Proof uses concentration inequality and stationary phase analysis.

- The pairwise coherence has the form

$$S_n = \frac{1}{n}\sum_{j=1}^{n} e^{i\omega \widehat{\mathbf{r}}_j\cdot(\mathbf{r}-\mathbf{r}')}$$

- Hoeffding inequality

$$\mathbb{P}\left[|S_n - \mathbb{E}S_n| \geq nt\right] \leq 2\exp\left[-\frac{nt^2}{2}\right]$$

  for all positive values of t.

- Expectation estimation:

$$\frac{1}{n}\mathbb{E}\left[\sum_{j=1}^{n} e^{i\omega \widehat{\mathbf{r}}_j\cdot(\mathbf{r}-\mathbf{r}')}\right] = \int_0^{2\pi} e^{i\omega \widehat{\mathbf{r}}\cdot(\mathbf{r}-\mathbf{r}')} f^{\mathrm{s}}(\theta)d\theta, \quad \widehat{\mathbf{r}} = (\cos\theta, \sin\theta)$$

  which is the Herglotz wave function with kernel f^{s}.

Operator norm bound

Theorem 5 (AF 2009)

For the SIMO measurement we have

$$\|\mathbf{\Phi}\|^2 \leq \frac{2m}{n}$$

with probability larger than

$$\left(1 - c_1\sqrt{\frac{n-1}{m}}\right)^{n(n-1)}$$

The probability bound is probably not optimal.

Multiple-scattering wave

Lippmann-Schwinger equation

$$u(\mathbf{r}_i) = u^{\mathsf{i}}(\mathbf{r}_i) + \omega^2 \sum_{j \neq i} G(\mathbf{r}_i, \mathbf{x}_j)\nu_j u(\mathbf{x}_j)$$

Let i_k be the indices for which $\nu(\mathbf{r}_{i_k}) \neq 0$. Define the illumination and full field vectors at the locations of the scatterers:

$$\begin{aligned} U^{\mathsf{i}} &= (u^{\mathsf{i}}(\mathbf{r}_{i_1}), ..., u^{\mathsf{i}}(\mathbf{r}_{i_s}))^T \in \mathbb{C}^s \\ U &= (u(\mathbf{r}_{i_1}), ..., u(\mathbf{r}_{i_s}))^T \in \mathbb{C}^s. \end{aligned}$$

Let $\mathbf{G}$ be the $s \times s$ matrix

$$\mathbf{G} = [(1 - \delta_{jl})G(\mathbf{r}_{i_j}, \mathbf{r}_{i_l})]$$

and $\mathcal{V}$ the diagonal matrix

$$\mathcal{V} = \mathrm{diag}(\nu_{i_1}, ..., \nu_{i_s}).$$

Lippmann-Schwinger equation can be written as

$$U = U^{\mathsf{i}} + \omega^2 \mathbf{G} \mathcal{V} U$$

or

$$U = U^{\mathrm{i}} + \omega^2 \mathbf{G} X$$

On the other hand,

$$X = \mathcal{V}\left(\mathbf{I} - \omega^2 \mathbf{G}\mathcal{V}\right)^{-1} U^{\mathrm{i}}.$$

Theorem 6 (AF 2009)

Suppose

$$\omega^{-2} \quad \textit{is not an eigenvalue of the matrix } \mathbf{G}\mathcal{V}$$

and

$$U^{\mathrm{i}} \quad \textit{is not orthogonal to any row vector of } \left(\mathbf{I} - \omega^2 \mathbf{G}\mathcal{V}\right)^{-1}.$$

Then the true target $\mathcal{V}$ is given by

$$\mathcal{V} = \mathrm{diag}\left[\frac{X}{\omega^2 \mathbf{G} X + U^{\mathrm{i}}}\right]$$

where the division is in the entry-wise sense (Hadamard product).

Near-field measurements

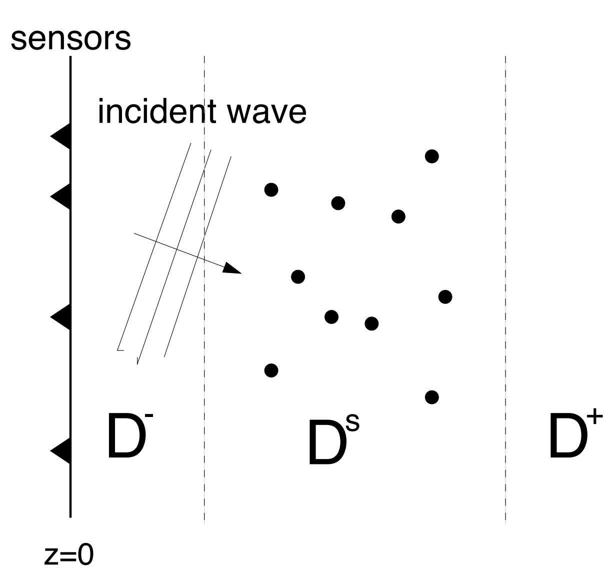

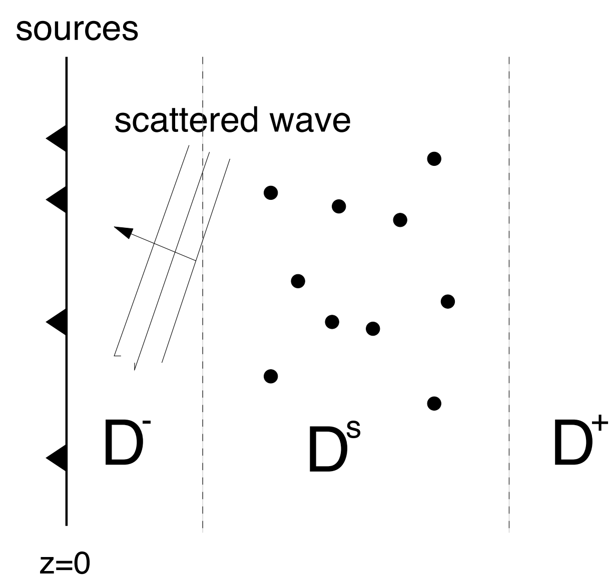

SIMO $\sim$ multi-shot SISO measurement.

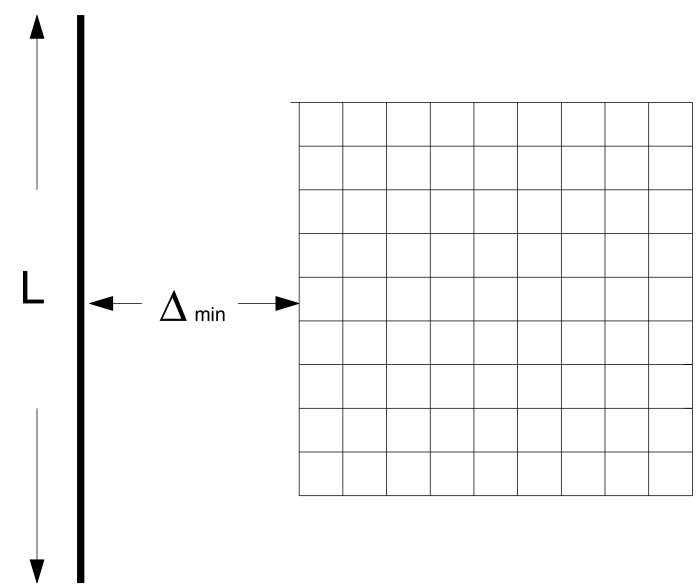

Theorem 7 *(AF 2009)*

Suppose

$$m \le \frac{\delta}{2} e^{2K^2/r_0^2}, \quad \delta > 0$$

where c_0 depends on the minimum distance Δ_{min} between $\{z = 0\}$ and the lattice (For $d = 2$, $r_0 = \mathcal{O}(-\log \Delta_{\text{min}})$; for $d = 3$, $r_0 = \mathcal{O}(\Delta_{\text{min}}^{-1})$).

The mutual coherence obeys

$$\begin{aligned} \mu(\Phi) &\le |G(\Delta_{\text{max}})|^{-2} \left(\frac{\sqrt{2}K}{\sqrt{n}} + \frac{c}{\sqrt{\omega L}} \right), \quad d = 2 \\ \mu(\Phi) &\le |G(\Delta_{\text{max}})|^{-2} \left(\frac{\sqrt{2}K}{\sqrt{n}} + \frac{c}{\omega L} \right), \quad d = 3 \end{aligned}$$

for some constant c (independent of $\omega > 0$ for $d = 2$ and $\omega > 1$ for $d = 3$), with probability greater than $(1 - \delta)^2$, where Δ_{max} is the largest distance between the array and the lattice.

Need $\omega L \gg 1$ and $n \gg 1$.

Resolution

$$\omega\ell \sim 1?$$

Multi-shot SISO schemes provide more information

Multi-shot SISO schemes

The (l, j)-entry of $\mathbf{\Phi} \in \mathbb{C}^{n\times m}$ is

$$\begin{aligned} e^{-i\omega_l \hat{\mathbf{r}}_l \cdot \mathbf{r}_j} e^{i\omega_l \hat{\mathbf{d}}_l \cdot \mathbf{r}_j} &= e^{i\omega_l \ell (j_2(\sin\theta_l - \sin\tilde{\theta}_l) + j_1(\cos\theta_l - \cos\tilde{\theta}_l))}, \\ & j = (j_1 - 1) + j_2. \end{aligned}$$

- Let $(\rho_l, \phi_l), i = 1, .., n$ be the polar coordinates of i.i.d. uniform r.v.s $(\xi_l, \eta_l) \in [0, 2\pi]^2$.

- **Scheme I.** This scheme employs $\Omega-$band limited probes, i.e. $\omega_l \in [-\Omega, \Omega]$. Set

$$\begin{aligned} \tilde{\theta}_l &= \theta_l + \pi = \phi_l \quad \text{(backward sampling)} \\ \omega_l &= \frac{\Omega \rho_l}{\sqrt{2}} \end{aligned}$$

  $l = 1, ..., n$. In this case the scattering amplitude is always sampled in the back-scattering direction analogous to SAR.

- **Scheme II.** This scheme employs single frequency probes no less than Ω:

$$\omega_l = \gamma\Omega, \quad \gamma \geq 1, \quad l = 1, ..., n.$$

Set

$$\begin{aligned} \theta_l &= \phi_l + \arcsin \frac{\rho_l}{\gamma\sqrt{2}} \\ \tilde{\theta}_l &= \phi_l - \arcsin \frac{\rho_l}{\gamma\sqrt{2}}. \end{aligned}$$

The difference between the incident angle and the sampling angle is

$$\theta_l - \tilde{\theta}_l = 2 \arcsin \frac{\rho_l}{\gamma\sqrt{2}} \quad \text{(scattering angles)}$$

which diminishes as $\gamma \to \infty$. In other words, in the high frequency limit, the sampling angle approaches the incident angle. This resembles the setting of the X-ray tomography.

- **Theorem 8** (AF 2009)

  Suppose

$$\Omega\ell = \pi/\sqrt{2}.$$

  Then scheme I and II satisfy RIP with high probability and the error bound

$$\|\hat{X} - X\|_2 \leq C_1 s^{-1/2} \|X - X^{(s)}\|_1 + C_2 \varepsilon.$$

Numerical tests

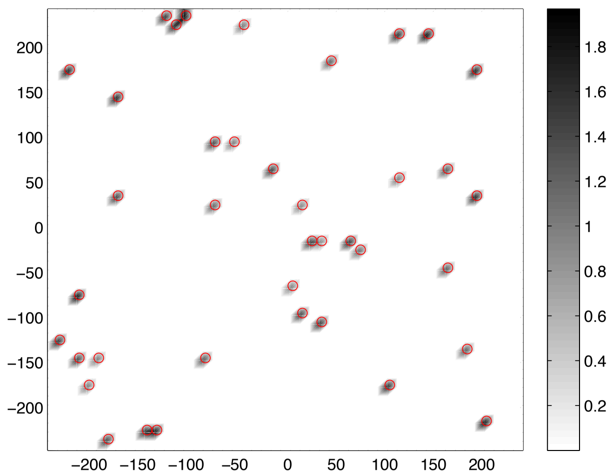

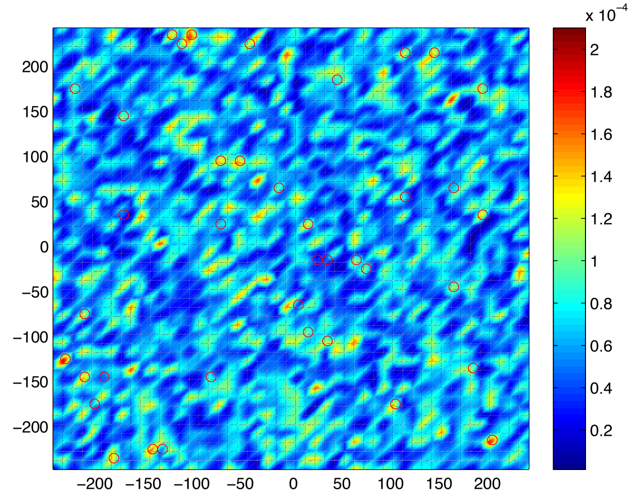

(left) Source inversion with the paraxial sensing matrix 40 source points and 121 antennas. The resulting error is 0.0164 while the error with exact Green function is 7×10^{-16} (not shown). (right) MFP image produced on the same grid. The red circles represent the true locations of the targets in both plots.

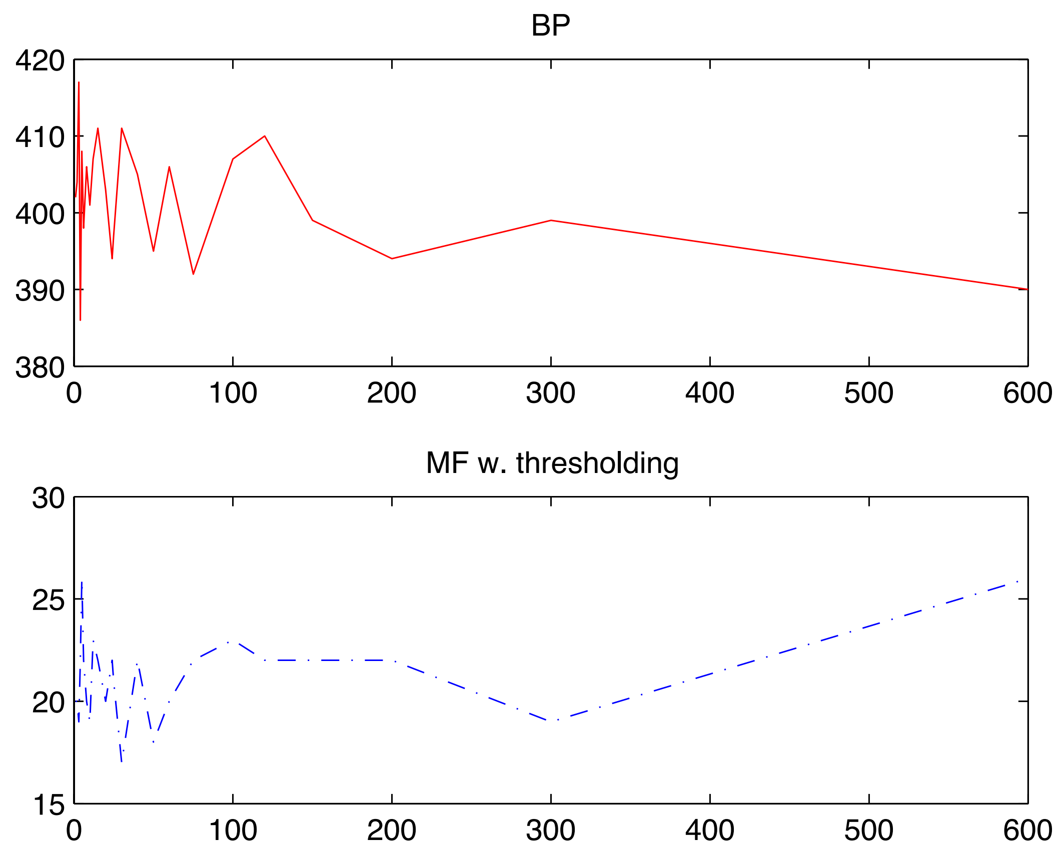

Compressed imaging by MFP (bottom) versus BP (top). The number of recoverable objects as a function of the number of sensors $n=$ 1,2,3,4,5, 6, 8, 10, 12, 15, 20, 24, 25, 30, 40, 50, 60, 75, 100, 120, 150, 200, 300, 600 with $np = 600$ fixed.

Scheme I: success probability

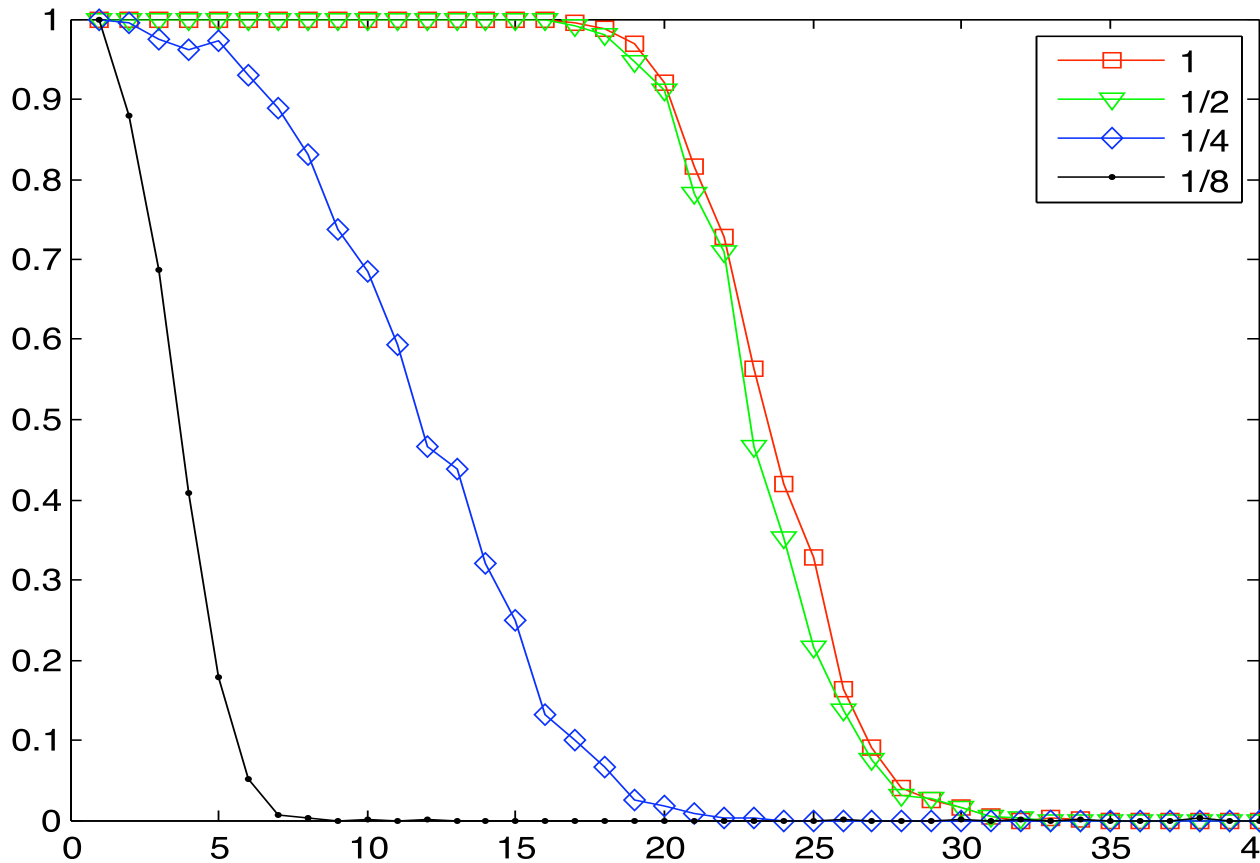

Success probabilities for Scheme I. As the backward sampling condition is increasingly violated, the performance degrades accordingly.

Scheme II: success probability

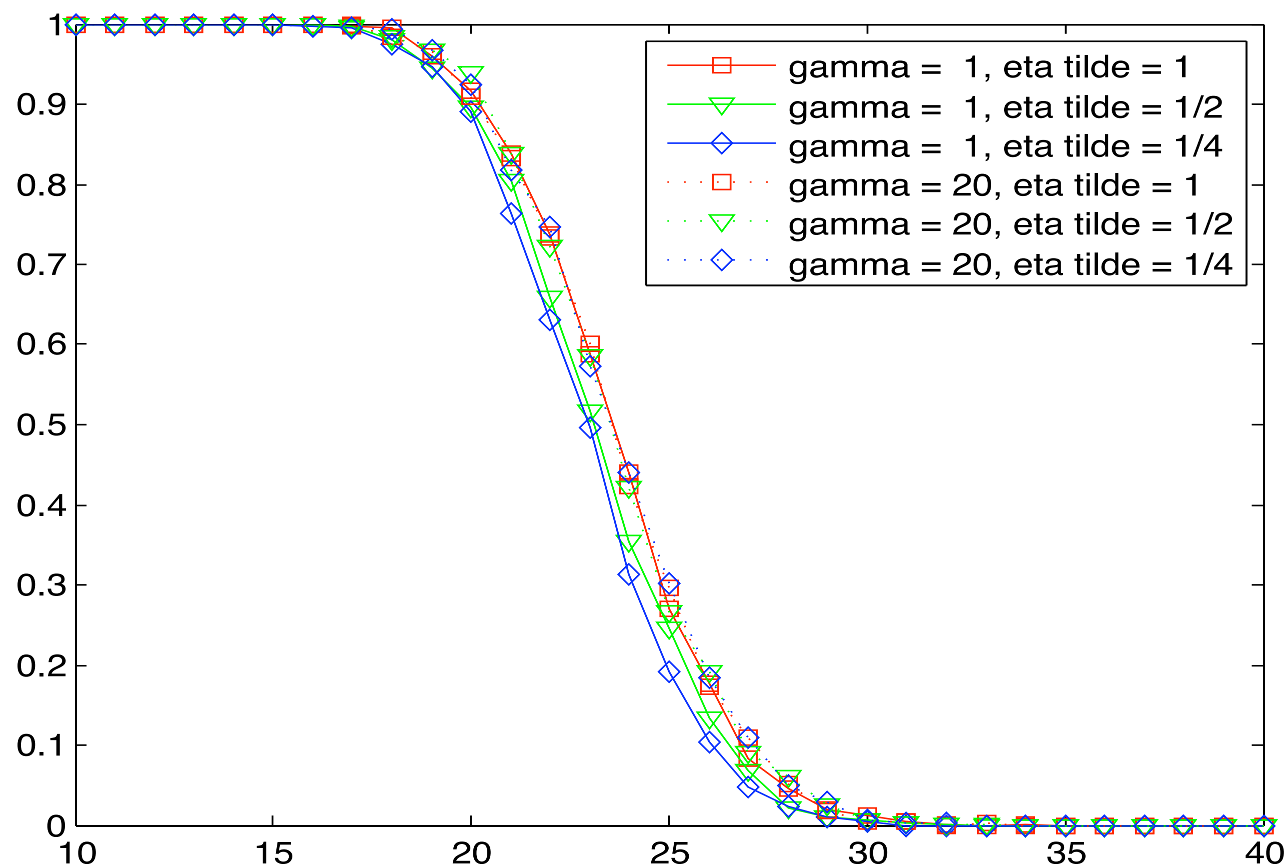

Success probabilities for Scheme II with $\gamma = 1, 20$ and the scattering angle condition violated in various degrees.

Comparison of SIMO and SISO

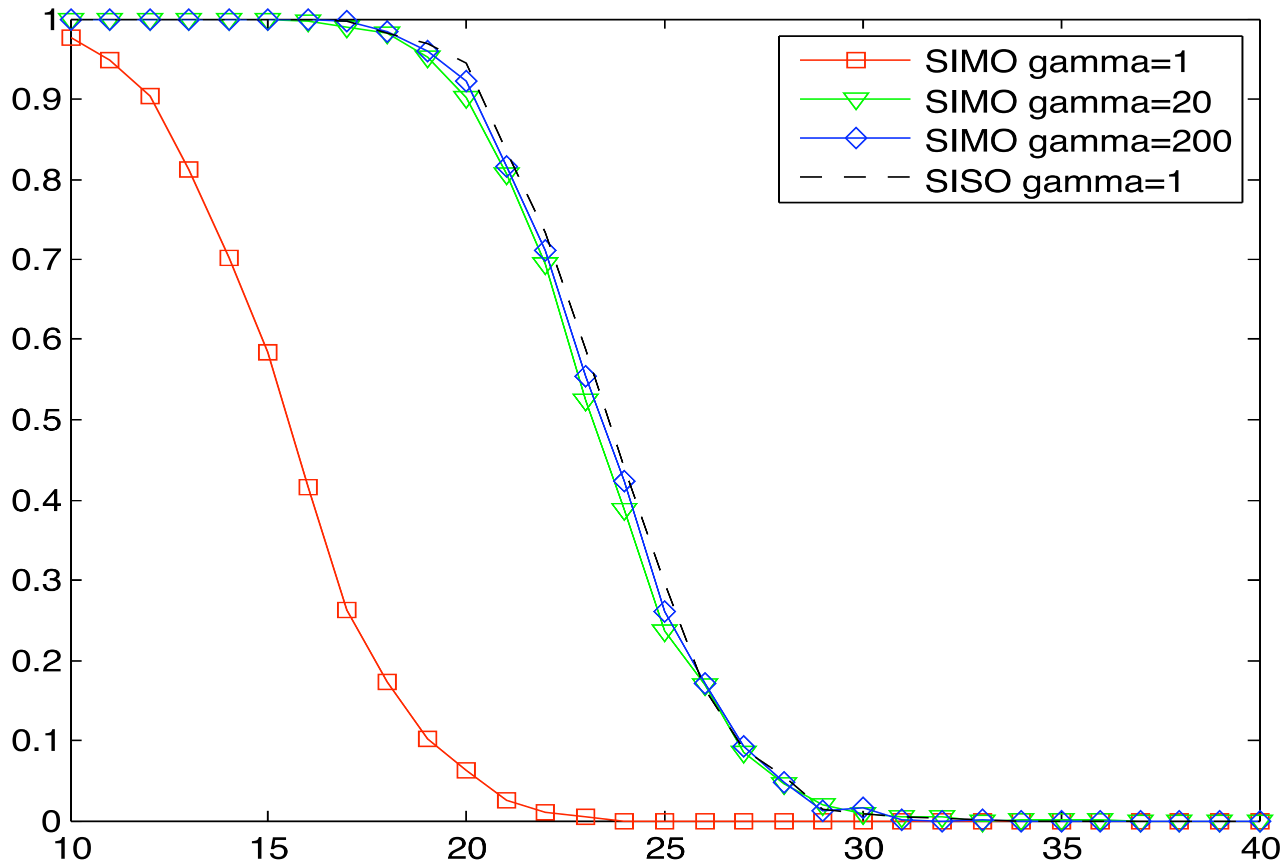

Solid curves are the success probabilities for the SIMO measurement at $\gamma = 1, 20, 200$ and the dashed curve is the SISO Scheme II at $\gamma = 1$.

Distributed extended targets

- The wavelet expansion

$$\nu(x,z) = \sum_{\mathbf{p},\mathbf{q}\in\mathbb{Z}^2} \nu_{\mathbf{p},\mathbf{q}}\psi_{\mathbf{p},\mathbf{q}}(x,z)$$

where

$$\psi_{\mathbf{p},\mathbf{q}}(\mathbf{r}) = 2^{-(p_1+p_2)/2}\psi(2^{-\mathbf{p}}\mathbf{r}-\mathbf{q}), \quad \mathbf{p},\mathbf{q}\in\mathbb{Z}^2$$

with

$$2^{-\mathbf{p}}\mathbf{r} = (2^{-p_1}x, 2^{-p_2}z)$$

form an ONB in $L^2(\mathbb{R}^2)$.

- Littlewood-Paley basis

$$\psi(\mathbf{r}) = (\pi^2 xz)^{-1}(\sin(2\pi x) - \sin(\pi x))\cdot(\sin(2\pi z) - \sin(\pi z))$$

which is band-limited

$$\widehat{\psi}(\xi,\zeta) = \begin{cases} (2\pi)^{-1}. & \pi \le |\xi|, |\zeta| \le 2\pi \\ 0, & \text{otherwise.} \end{cases}$$

- With the incident fields

$$u^{\mathrm{i}}_k(\mathbf{r}) = e^{i\omega_k \mathbf{r}\cdot\hat{\mathbf{d}}_k}, \quad k = 1, ..., n$$

  we have

$$Y_k = 2\pi \sum_{\mathbf{p},\mathbf{q}\in\mathbb{Z}^2} 2^{(p_1+p_2)/2} \nu_{\mathbf{p},\mathbf{q}} e^{i\omega_k 2^{\mathbf{p}}(\hat{\mathbf{d}}_k-\hat{\mathbf{r}}_k)\cdot\mathbf{q}} \widehat{\psi}(\omega_k 2^{\mathbf{p}}(\hat{\mathbf{r}}_k - \hat{\mathbf{d}}_k))$$

  with cutoffs

$$|\mathbf{q}|_\infty \le m_{\mathbf{p}}, \quad |\mathbf{p}|_\infty \le p_*, \quad |\mathbf{q}'|_\infty \le n_{\mathbf{p}'}, \quad |\mathbf{p}'|_\infty \le p_*.$$

- Let

$$l = \sum_{\substack{j_1=-p_*\\ |\mathbf{q}|_\infty \le m_{\mathbf{p}},}}^{p_1-1} \sum_{\substack{j_2=-p_*\\ |\mathbf{p}|_\infty \le p_*,}}^{p_2-1} (2m_{\mathbf{j}}+1)^2 + (q_1+m_{\mathbf{p}})(2m_{\mathbf{p}}+1) + (q_2+m_{\mathbf{p}}+1),$$

$$k = \sum_{\substack{j_1=-p_*\\ |\mathbf{q}'|_\infty \le n_{\mathbf{p}'},}}^{p'_1-1} \sum_{\substack{j_2=-p_*\\ |\mathbf{p}'|_\infty \le p_*.}}^{p'_2-1} (2n_{\mathbf{j}}+1)^2 + (q'_1+n_{\mathbf{p}'})(2n_{\mathbf{p}'}+1) + (q'_2+n_{\mathbf{p}'}+1),$$

Define the sensing matrix elements to be

$$\Phi_{k,l} = \frac{1}{2n_{\mathbf{p}}+1}\widehat{\psi}(\omega_k 2^{\mathbf{p}}(\hat{\mathbf{r}}_k - \hat{\mathbf{d}}_k))e^{i\omega_k 2^{\mathbf{p}}(\hat{\mathbf{d}}_k - \hat{\mathbf{r}}_k)\cdot\mathbf{q}}$$

and let $\mathbf{\Phi} = [\Phi_{k,l}]$, where $\hat{\mathbf{d}}_k, \hat{\mathbf{r}}_k, \omega_k$ are given below.

Let $X = (X_l)$ with

$$X_l = 2\pi(2n_{\mathbf{p}}+1)2^{(p_1+p_2)/2}\nu_{\mathbf{p},\mathbf{q}}$$

be the target vector.

- Sampling scheme:

  Let ξ_k, ζ_k be independent, uniform random variables on $[-1,1]$ and define

$$\alpha_k = \frac{\pi}{\omega_k 2^{p_1'}} \cdot \begin{cases} 1+\xi_k, & \xi_k \in [0,1] \\ -1+\xi_k, & \xi_k \in [-1,0] \end{cases}$$

$$\beta_k = \frac{\pi}{\omega_k 2^{p_2'}} \cdot \begin{cases} 1+\zeta_k, & \zeta_k \in [0,1] \\ -1+\zeta_k, & \zeta_k \in [-1,0] \end{cases}.$$

  Let (ρ_k, ϕ_k) be the polar coordinates of (α_k, β_k) used to define schemes I and II.

- $\Phi_{k,l}$ are zero if $\mathbf{p} \neq \mathbf{p}'$. Consequently the sensing matrix is the block-diagonal matrix with each block (indexed by $\mathbf{p} = \mathbf{p}'$) in the form of random Fourier matrix

$$\Phi_{k,l} = \frac{1}{2n_{\mathbf{p}}+1} e^{i\pi(q_1\xi_k + q_2\zeta_k)}.$$

  The above observation means that the target structures of different dyadic scales are decoupled and can be determined separately by our approach using compressed sensing techniques.

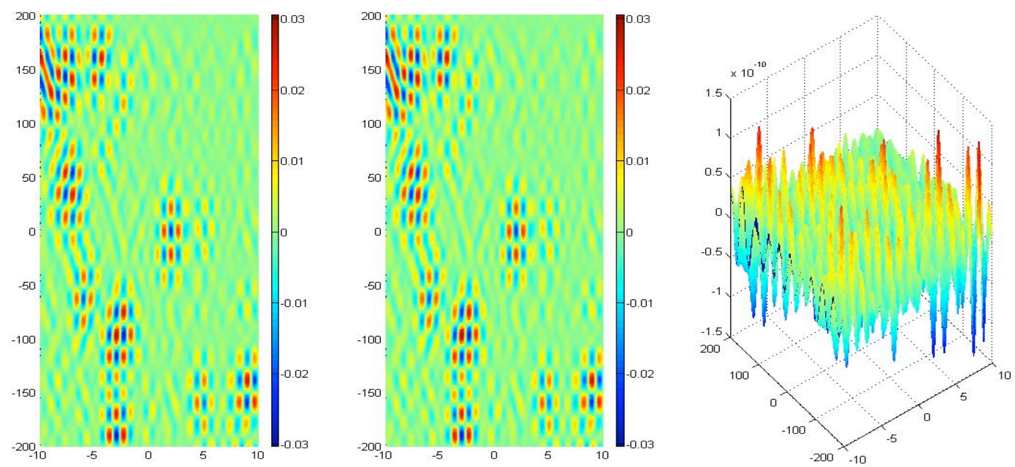

Imaging of an extended target of the scales $p_* = 0$ with $m_0 = 32$.

Localized extended targets

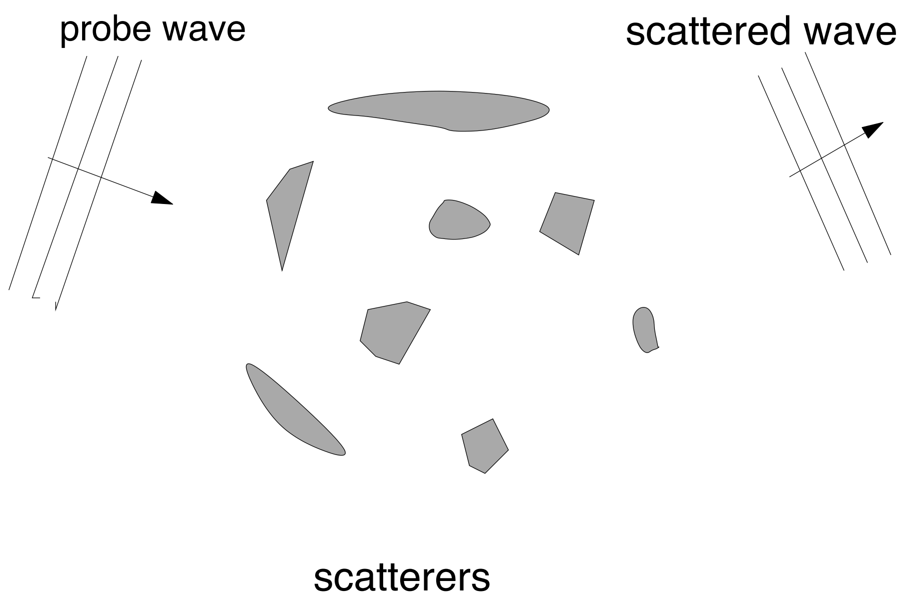

- Interpolation from the grid

$$\nu_\ell(\mathbf{r}) = \ell^2 \sum_{\mathbf{q}\in I} g(\frac{\mathbf{r}}{\ell} - \mathbf{q})\nu(\ell\mathbf{q}), \quad I \subset \mathbb{Z}^2.$$

$$Y = \mathbf{\Phi} X + E$$

where E includes the discretization error.

Theorem 9 (AF 2009)

Consider the sampling schemes I and II (with $\gamma = 1$). In addition to the previous assumptions assume

$$\|\nu - \nu_\ell\|_1 \leq \frac{2\pi\varepsilon}{\|\widehat{g}^{-1}\|_{L^\infty([-\pi,\pi]^2)}}.$$

Then schemes I and II satisfy RIP with high probability and the error bound

$$\|\hat{X} - X\|_2 \leq C_1 s^{-1/2} \|X - X^{(s)}\|_1 + C_2 \varepsilon.$$

Random illumination

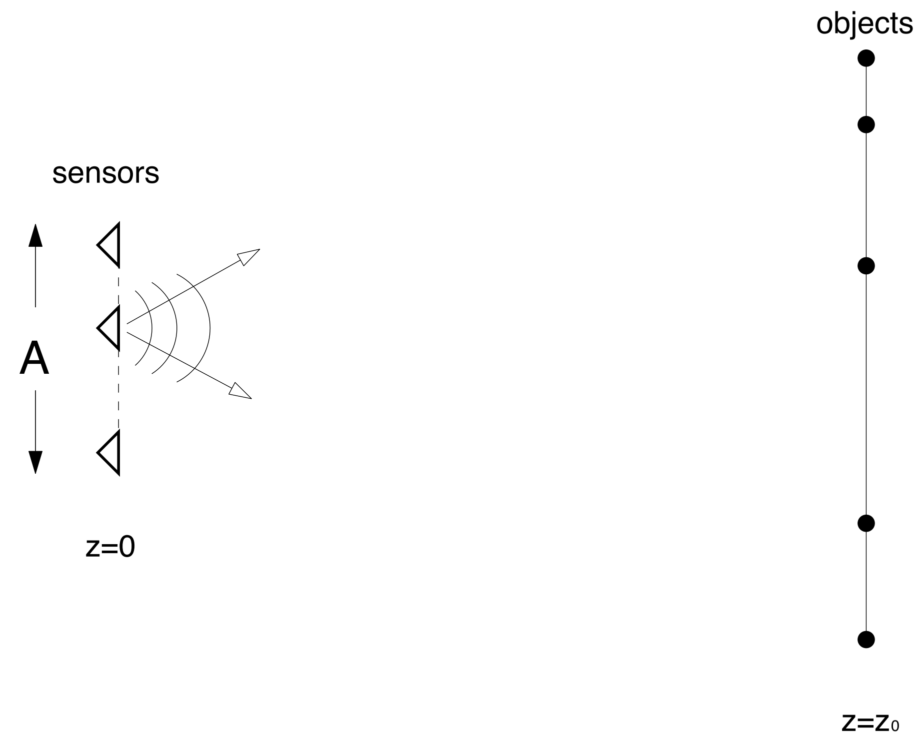

- Rayleigh resolution:

$$\frac{A\ell}{z_0\lambda} = \mathcal{O}(1)$$

- Paraxial Green function G

$$G_{\text{par}}(\mathbf{r},\mathbf{a}) = \frac{e^{i\omega z_0}}{4\pi z_0} e^{i\omega|x-\xi|^2/(2z_0)} e^{i\omega|y-\eta|^2/(2z_0)}, \quad \mathbf{r} = (x,y,z_0), \quad \mathbf{a} = (\xi,\eta,$$

- *Random* illumination u^{i}. Assume we have a full control of the source points in $\{(x,y,z) : x,y \in [-L/2, L/2], z = z_1\}$ and write the incident wave as

$$u^{\mathrm{i}}(\mathbf{r}) = \int_{-L/2}^{L/2}\int_{-L/2}^{L/2} G_{\mathrm{par}}(\mathbf{r},(\xi,\eta,z_1))f(\xi,\eta)d\xi d\eta$$

- Let the source distribution f be a complex-valued, circularly symmetric Gaussian white-noise field of variance κ^2:

$$\begin{aligned}\mathbb{E}\left[f(\xi,\eta)f^*(\xi',\eta')\right] &= \kappa^2\delta(\xi-\xi',\eta-\eta')\\ \mathbb{E}\left[f(\xi,\eta)f(\xi',\eta')\right] &= 0, \quad \forall \xi,\xi',\eta,\eta'.\end{aligned}$$

- Fresnel transformation is unitary and hence u^{i} is also a complex-valued, circularly symmetric Gaussian random field.

  The random incident field takes on i.i.d. random values at grid points. Since the incident field has the same magnitude throughout the object plane, after normalization its effect at the grid points can be represented by a phase factor $e^{i\theta_j}, j = 1, ..., N$

where θ_j are i.i.d uniform random variables in $[0, 2\pi]$ (i.e. circularly symmetric).

- **Theorem 10** *Suppose*

$$\frac{aK\sqrt{2}}{\sqrt{p}} + \frac{2K^2}{\sqrt{np}} \le \frac{a_0}{\log N}$$

where

$$a = \max_{j \neq j'} \left| \mathbb{E}\left(e^{i\xi_l \omega(x_{j'} - x_j)/z_0}\right) \mathbb{E}\left(e^{i\eta_l \omega(y_{j'} - y_j)/z_0}\right) \right|.$$

Assume that the s objects are real-valued and satisfy

$$X_{\min} > 8\sigma\sqrt{2\log N}$$

and

$$s \le \frac{c_0 np}{2\log N}.$$

Then the Lasso estimate $\hat{X}$ with $\gamma = 2\sqrt{2\log N}$ has the same support as X with probability at least

$$1 - 2\delta - \rho n(n-1)\frac{\pi}{2}\sqrt{\frac{np-1}{N}} - 2n^2 p(p-1)e^{-\frac{N}{(np-1)^2}}$$
$$-2N^{-1}((2\pi\log N)^{-1/2} + sN^{-1}) - \mathcal{O}(N^{-2\log 2})).$$

The superresolution effect can occur when the number p of random probes is large. Consider, for example, the case of $n = 1$ and hence the aperture A is essentially zero. Since $a \leq 1$, the condition

$$\frac{K\sqrt{2} + 2K^2}{\sqrt{p}} \leq \frac{a_0}{\log N}$$

and

$$s \leq \frac{c_0 p}{2 \log N}$$

implies that the Lasso with $\gamma = 2\sqrt{2 \log N}$ recovers exactly the support of s objects.

Numerical results with RI

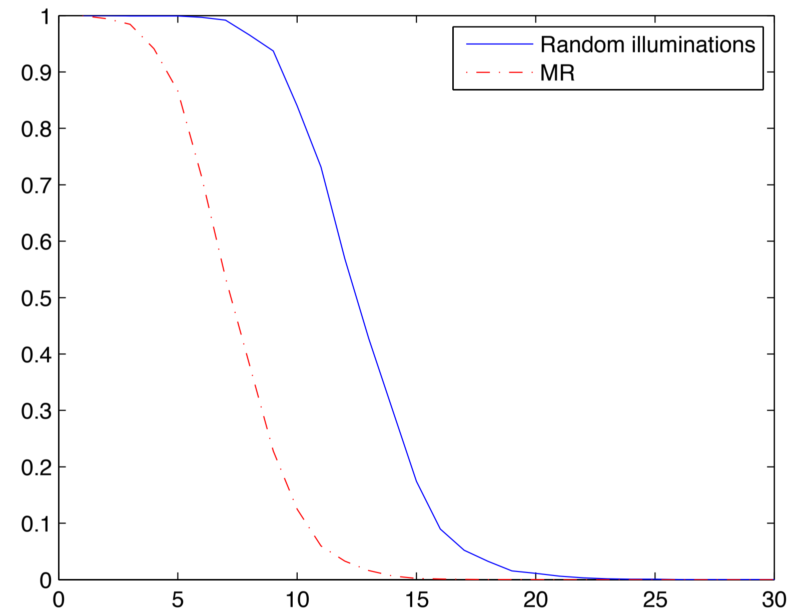

The Lasso performance comparison between RI with $n = 11, p = 6$ and MR with $n = 11$. The vertical axis is for the success probability and the horizontal axis is for the number of objects. The success probability is estimated from 1000 independent trials.

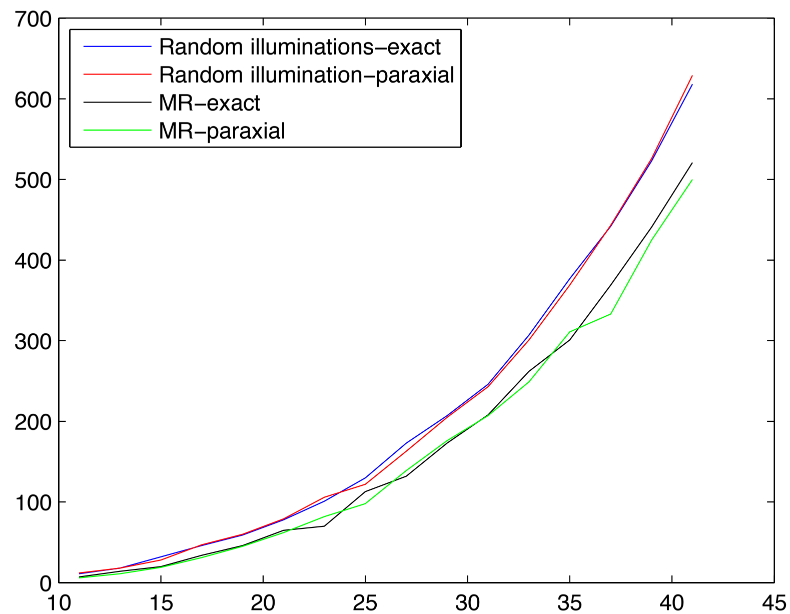

The numbers of recoverable (by the Lasso) objects for RI with $p = (n+1)/2$ and MR as n varies. The curves indicate a quadratic behavior predicted by the theory. The difference between recoveries with the exact and paraxial Green functions is negligible in both the RI and MR set-ups.

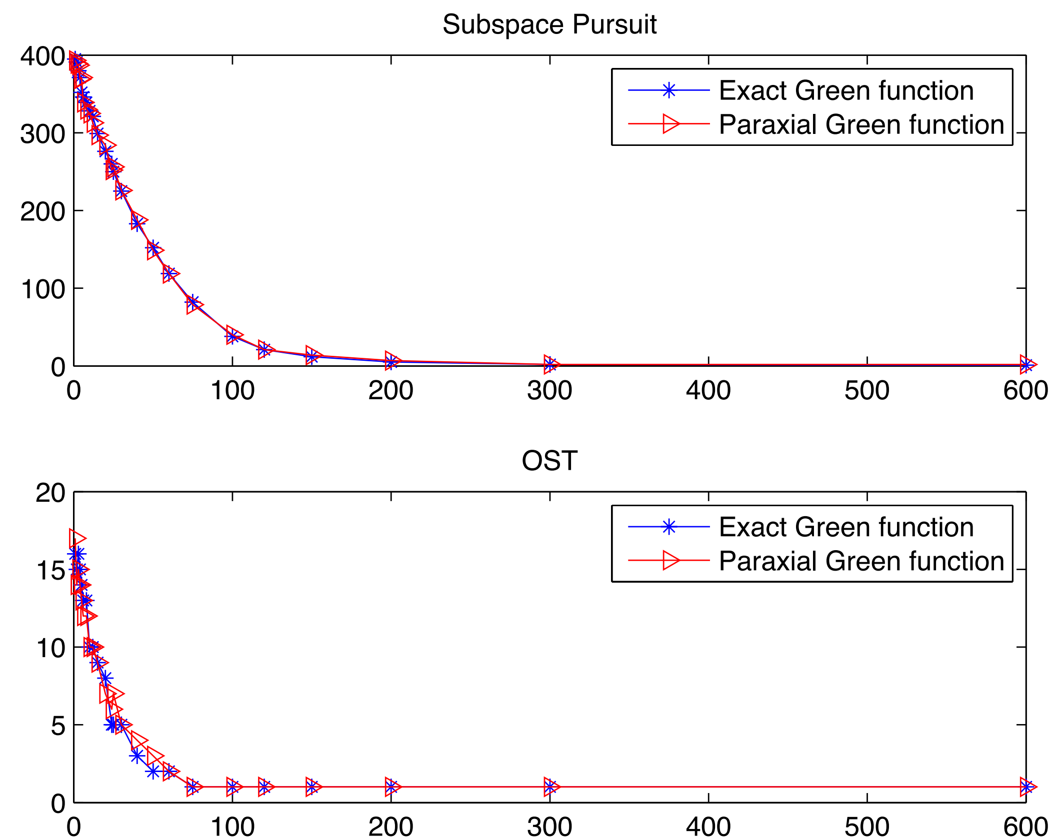

The number of recoverable objects in the under-resolved case as a function of the number of sensors $n = 1,2,3,4,5,\ 6,\ 8,\ 10,\ 12,\ 15,\ 20,\ 24,\ 25,\ 30,\ 40,\ 50,\ 60,\ 75,\ 100,\ 120,\ 150,\ 200,\ 300,\ 600$ with $np = 600$ fixed.

MUSIC algorithm

- Define the data matrix $\mathbf{Y} = (Y_{k,l}) \in \mathbb{C}^{n\times m}$ as

$$Y_{k,l} \sim A(\hat{\mathbf{s}}_k, \hat{\mathbf{d}}_l), \quad k = 1, ..., n, \quad l = 1, ..., m$$

  where we keep open the option of normalizing $\mathbf{Y}$ in order to simplify the set-up. The data matrix is related to the object matrix

$$\mathbf{X} = \text{diag}(\xi_j) \in \mathbb{C}^{s\times s}, \quad j = 1, ...s$$

  by the measurement matrices $\mathbf{\Phi}$ and $\mathbf{\Psi}$ as

$$\mathbf{Y} = \mathbf{\Phi X \Psi}^*$$

  where $\mathbf{\Phi}$ and $\mathbf{\Psi}$ are, respectively,

$$\begin{aligned} \Phi_{k,j} &= \frac{1}{\sqrt{n}} e^{-i\omega \hat{\mathbf{s}}_k \cdot \mathbf{r}_j} \in \mathbb{C}^{n\times s} \\ \Psi_{l,j} &= \frac{1}{\sqrt{n}} e^{-i\omega \hat{\mathbf{d}}_l \cdot \mathbf{r}_j} \in \mathbb{C}^{m\times s}. \end{aligned}$$

- The standard version of MUSIC algorithm deals with the case of $n = m$ and $\hat{\mathbf{s}}_k = \hat{\mathbf{d}}_k, k = 1, ..., n$ as stated in the following result.

Proposition 2 *(Kirsch 02, 08) Let $\{\hat{\mathbf{s}}_k = \hat{\mathbf{d}}_k, k \in \mathbb{N}\}$ be a countable set of directions such that any analytic function on the unit sphere that vanishes in $\hat{\mathbf{s}}_k, \forall k \in \mathbb{N}$ vanishes identically. Let $\mathcal{K} \subset \mathbb{R}^3$ be a compact subset containing $\mathcal{S}$. Then there exists n_0 such that for any $n \geq n_0$ the following characterization holds for every $\mathbf{r} \in \mathcal{K}$:*

$$\mathbf{r} \in \mathcal{S} \quad \text{if and only if} \quad \phi_{\mathbf{r}} \equiv \frac{1}{\sqrt{n}}(e^{-i\omega\hat{\mathbf{s}}_1\cdot\mathbf{r}}, e^{-i\omega\hat{\mathbf{s}}_2\cdot\mathbf{r}}, \cdots, e^{-i\omega\hat{\mathbf{s}}_n\cdot\mathbf{r}})^T \in \mathrm{Ran}(\mathbf{\Phi}).$$

Moreover, the ranges of $\mathbf{\Phi}$ and $\mathbf{Y}$ coincide.

Remark 1 *As a consequence, $\mathbf{r} \in \mathcal{S}$ if and only if $\mathcal{P}\phi_{\mathbf{r}} = 0$ where $\mathcal{P}$ is the orthogonal projection onto the null space of $\mathbf{Y}^*$ (Fredholm alternative). And the locations of the scatterers can be identified by the singularities of the imaging function*

$$J(\mathbf{r}) = \frac{1}{|\mathcal{P}\phi_{\mathbf{r}}|^2}.$$

- **Theorem 11** *Suppose $\delta_{s+1} < 1$ and $\|\mathbf{E}\|_2 = \varepsilon$.*

The thresholding rule then the object support $\mathcal{S}$ can be identified by the thresholding rule

$$\left\{\mathbf{r} \in \mathcal{K} : J^{\varepsilon}(\mathbf{r}) \geq 2\left(1 - \frac{\delta_{s+1}(1+\delta_s)}{2+\delta_s-\delta_{s+1}}\right)^{-2}\right\}$$

under the following bound on the noise-to-scatterer ratio (NSR)

$$\frac{\varepsilon}{\xi_{\min}} < \sqrt{(1+\delta_s)^2\frac{\xi_{\max}^2}{\xi_{\min}^2} + (1-\delta_s)^2\Delta} - (1+\delta_s)\frac{\xi_{\max}}{\xi_{\min}}$$

where

$$\Delta = \min\left\{\nu_*\left(\frac{(1+\delta_s)^2}{(1-\delta_s)^2}\frac{\xi_{\max}^2}{\xi_{\min}^2}\right), \frac{1}{5\sqrt{2}}\left(1 - \frac{\delta_{s+1}(1+\delta_s)}{2+\delta_s-\delta_{s+1}}\right)\right\}$$

$$\nu_*(x) = \frac{-2x-1+\sqrt{(2x+1)^2+16}}{16}$$

and $\xi_{\max}/\xi_{\min}$ *is the dynamic range of scatterers.*

MUSIC simulations

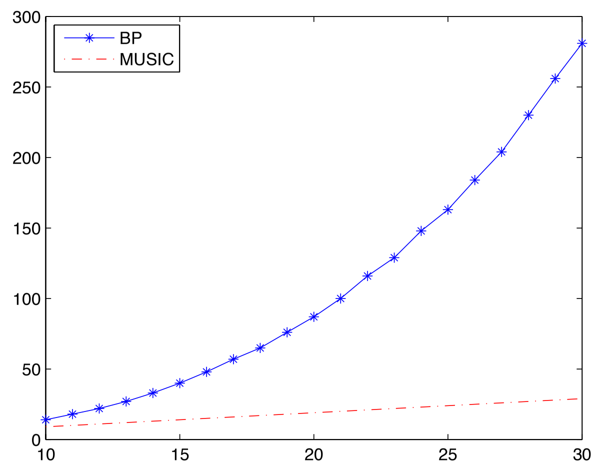

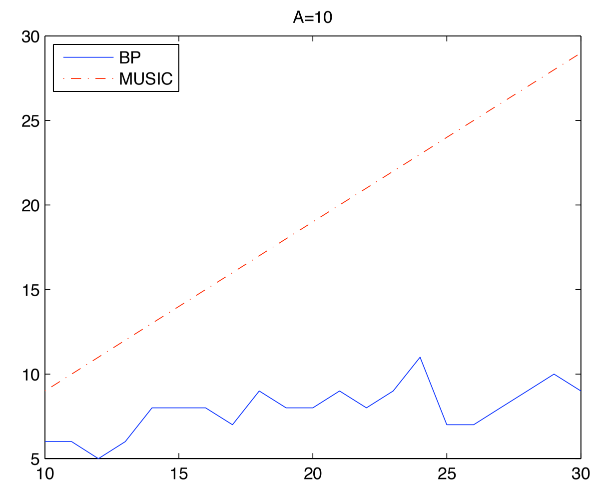

Comparison of MUSIC and BP performances, with both using the whole data matrix: the number s of recoverable scatterers versus the number of sensors n with $A = 100$ (left), the well-resolved case, and $A = 10$ (right), the under-resolved case. In the well-resolved case, BP delivers a much better (quadratic-in-n) performance than MUSIC; in the under-resolved case, MUSIC outperforms BP whose performance tends to be unstable in this regime. The numbers of recoverable scatterers by BP are calculated based on successful recovery of at least 90 out of 100 independent realizations of transceivers and scatterers while the success rate of MUSIC is 100%.

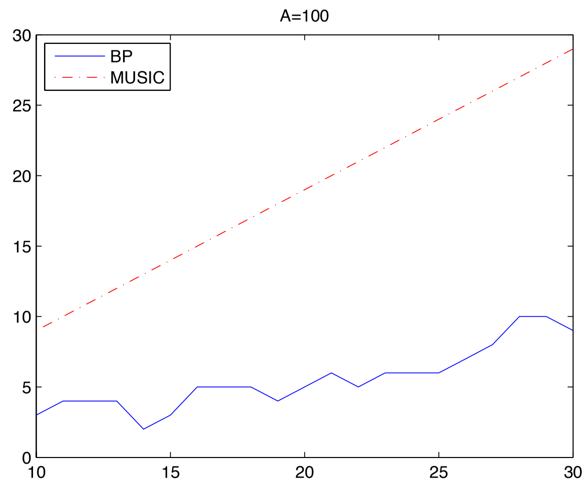

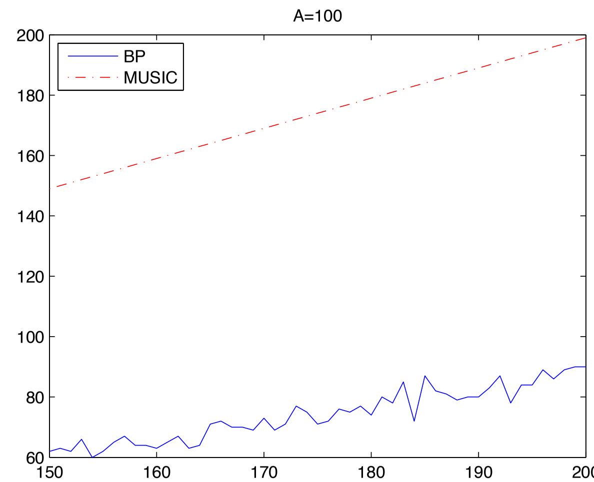

Comparison of MUSIC and BP performances with BP employing only *single* column of the data matrix: the number s of recoverable scatterers versus the number of sensors n with $A = 100$ for $n \in [10, 30]$ (left) and $n \in [150, 200]$ (right). Both BP curves show a roughly linear behavior with slope less than that of the MUSIC curves.

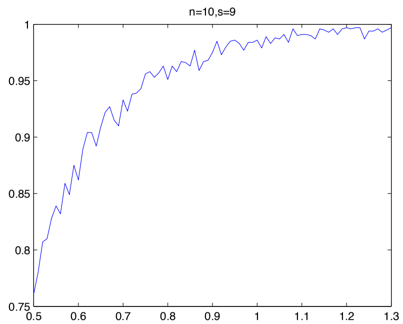

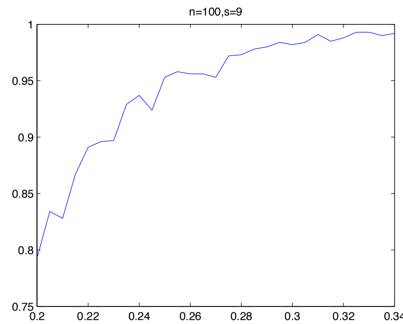

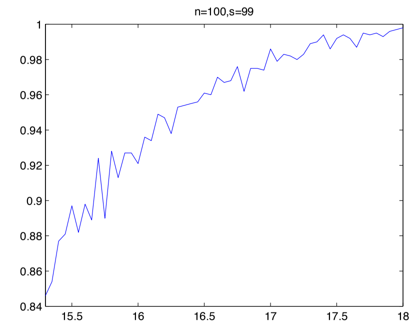

Success probability of the MUSIC reconstruction versus aperture for $n = 10, s = 9$ (left), $n = 100, s = 9$ (middle) and $n = 100, s = 99$ (right). Note the different aperture ranges for the three plots. The success rate is calculated from 1000 trials. Increasing the number of transceivers for the same number of scatterers reduces the aperture required for the same success rate. The reduction of aperture is about three folds (left to middle). On the other hand, higher number of scatterers with the same number of transceivers also demands larger aperture for the same success rate. The increase in aperture is about 7 times (middle to right).

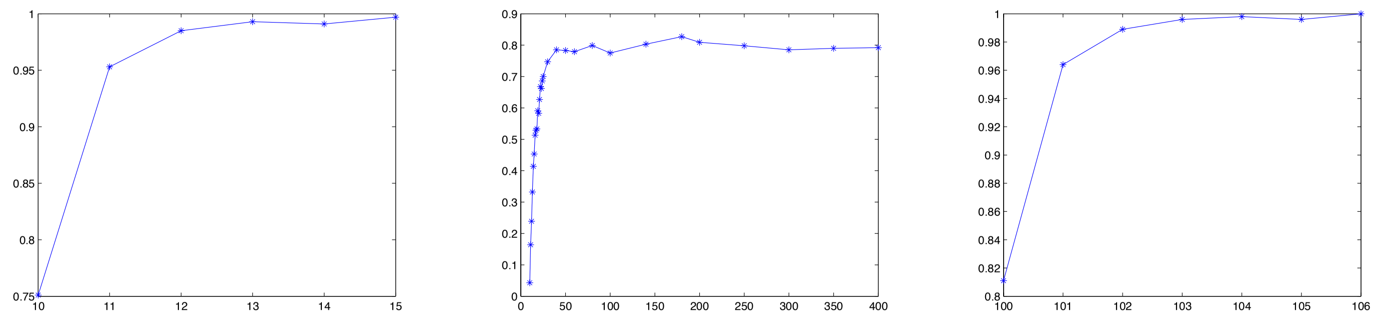

Success probability of MUSIC versus the number of transceivers with $A = 0.5, s = 9$ (left), $A = 0.2, s = 9$ (middle) and $A = 15, s = 99$ (right). The probabilities are calculated from 1000 independent trials.

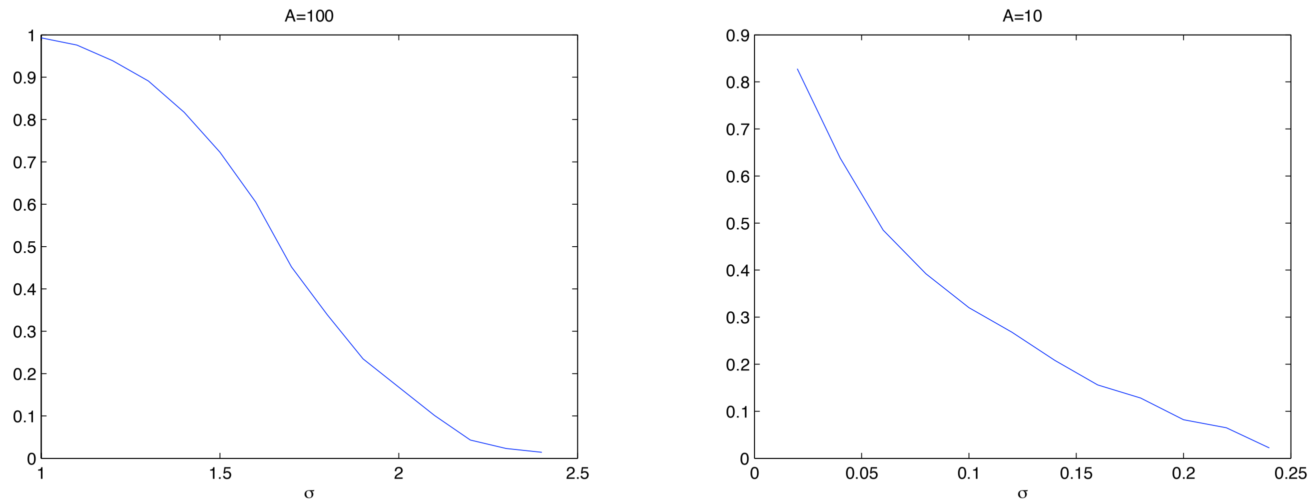

Success probability of MUSIC reconstruction of $s = 10$ scatterers with $n = 100$ transceivers versus the noise level σ in the well-resolved case $A = 100$ (left) and the under-resolved case $A = 10$ (right). The success rate is calculated from 1000 trials. Note the different scales of σ in the two plots. Noise sensitivity increases dramatically in the under-resolved case.

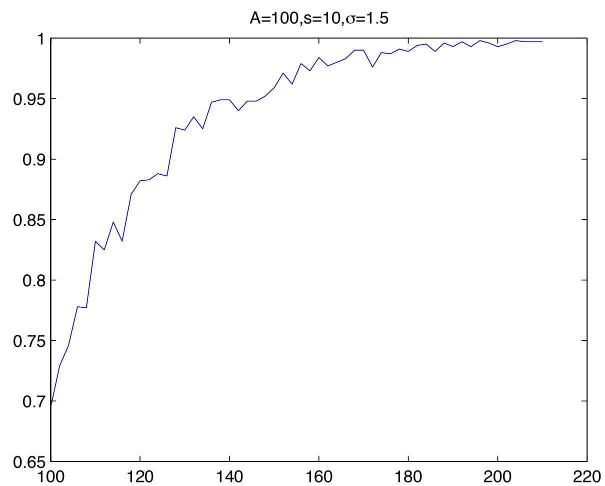

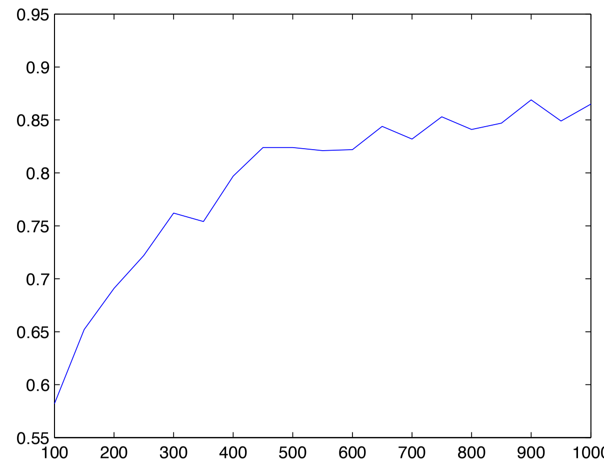

Success probability of MUSIC reconstruction of $s = 10$ scatterers as a function of n with $\sigma = 150\%$ in the well-resolved case $A = 100$ (left) and $\sigma = 5\%$ in the under-resolved case $A = 10$ (right). The success rate reaches the plateau of 85% near $n = 1000$ in the under-resolved case. The success rate is calculated from 1000 trials.

references

- A. F.: Compressive inverse scattering II. Multi-shot SISO measurements with Born scatterers *Inverse Problems* **26** (2010), 035009
- A. F.: Compressive inverse scattering I. high-frequency SIMO/MISO and MIMO measurements *Inverse Problems* **26** (2010), 035008
- A. F., P. Yan and T. Strohmer: Compressed Remote Sensing of Sparse Object. *SIAM J. Imaging Sci.* Volume 3, Issue 3, pp. 595-618 (2010).
- A. F.: Exact Localization and Superresolution with noisy data and random illumination `arXiv:1008.3146`
- A. F.: The MUSIC algorithm for sparse objects: a compressed sensing analysis `arXiv:1006.1678`

Conclusions

- Inverse scattering in the framework of compressed sensing.
- Random incident and scattering directions
- Random illumination
- Superresolution

THANK YOU!